# X-ray diffraction-based estimation of remaining fatigue life in AA6061-T6 for "additive remanufacturing""

Sepehr Ghazimorady<sup>1</sup>\*, Sina Negarandeh<sup>2</sup>, Yi Chen<sup>2</sup>, Melika Morafegh<sup>2</sup>, Verena Kantere<sup>2</sup>, Hamid Jahed<sup>1</sup>
<sup>1</sup> Fatigue & Stress Analysis Laboratory, Department of Mechanical & Mechatronics Engineering, University of Waterloo, 200 University Ave W, Waterloo, ON, N2L 3G1, Canada

Abstract: Cold spray is an advanced additive manufacturing technology that is capable of restoration of damaged metallic components without exposing them to high temperatures. To expand the use of cold spray from restoring the geometry and structure of defective parts to full remanufacturing, extending their lifespan beyond the original life cycle by replacing internally damaged areas (typically only 10–15% of the part's volume), the first step is to accurately assess the damage at the part's hot spot. This study explores the capabilities of X-ray diffraction (XRD) as a non-destructive testing method for assessing damage in AA6061-T6. A set of dog-bone samples was prepared to introduce controlled damage at different levels. X-ray diffraction measurements were conducted on these samples to generate test data, to assess dislocation densities. These values offer a quantified measure of internal damage and provide insight into the microstructural evolution under fatigue loading. By using this method, this study aims to develop a reliable method for pre-additive remanufacturing® damage assessment. In corroboration with earlier studies, we show that XRD can effectively detect internal material damage using dislocation densities through XRD-measured parameters such as full width at half maxima (FWHM), a measure of XRD peak broadening used for analyzing dislocation and strain. Integrating XRD-based damage assessment with cold spray additive manufacturing can enable precise and localized repairs. By implementing cold spray remanufacturing, this method can significantly reduce material waste, a major contributor to the greenhouse gas emissions, and extend components' lifespans across various industries, promoting sustainability and circular economy.

**Keywords:** additive remanufacturing<sup>®</sup>, cold spray, fatigue damage assessment, sustainability, XRD

#### 1. Introduction

Cold spray (CS) technology has become increasingly important in additive remanufacturing due to its ability to restore components without thermally affecting the material. It enables the deposition of metallic coatings and layers by accelerating particles to speeds exceeding sound velocity in air and embedding them into the substrate via solid-state deformation. This low-temperature process preserves the mechanical properties of the material, making it ideal for repairing defective parts, by restoring damaged areas [1]. However, to fully utilize CS for functional remanufacturing, extension of parts life at the end of its life cycle, it is necessary to assessing the damage at the hot spots of load bearing parts. Components subjected to fatigue typically fail due to damage accumulation in localized regions caused by stress concentrations. Thus, detecting where damage occurs and assessing the remaining life enables selective, and localized fatigue life enhancement, extending the overall fatigue life of the component for an additional cycle. This approach results in significant material and energy savings while minimizing cost and environmental impact.

X-ray diffraction (XRD) has emerged as a powerful, non-destructive technique for internal damage assessments. Under cyclic mechanical loading, materials experience deformation, dislocation accumulation, and lattice strain, all of which affect XRD patterns. Several studies have confirmed that fatigue causes XRD peak to shift and broaden [2-4]. This causes the value of the full width at half maximum (FWHM) change with the fatigue damage state of the material [5-7]. These peak shifts correspond closely with microstructural strain and damage evolution, validating XRD's role as a fatigue damage assessment. Uniform deformation of the microstructure results in a shift of the diffraction peak position, while non-uniform deformation in the microstructure leads to peak broadening, which is typically observed as an increase in FWHM [8]. Traditionally, most research has focused on tracking one or two of the XRD peak parameters, typically FWHM, and establishing its relationship with fatigue life [7, 9]. While useful, this approach does not fully leverage the information embedded in the complete diffraction pattern. In parallel with the present experimental work, we have also developed a dataset that includes all extracted XRD parameters as well as the corresponding raw diffraction images. Although machine learning implementation is beyond the scope of this study, this dataset has been specifically structured for future work in which machine learning techniques may be applied to identify patterns in the data and improve

<sup>&</sup>lt;sup>2</sup> Modern Management of Data and Analytics Lab, School of Electrical Engineering and Computer Science, Faculty of Engineering, University of Ottawa.

<sup>\*</sup>Corresponding author's email address: sghazimo@uwaterloo.ca

1 2 (a)

predictive capabilities. The ultimate goal is to assess damage and guide targeted material removal and remanufacturing through the cold spray method.

#### 2. Material and methods

# 2.1 Sample preparation and fatigue testing

93.4

The test material used in this study is AA6061-T6 aluminum alloy, a widely used material in automotive components due to its favorable mechanical properties and corrosion resistance. Standard dog-bone shaped specimens were machined from  $25.4 \times 25.4$  mm extruded blocks. The exact dimensions of the specimens are shown in

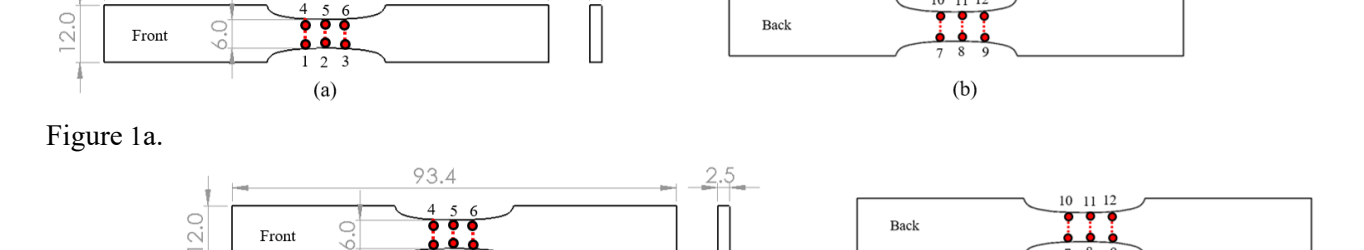


Figure 1: The geometry of the dog bone samples (units in mm) and the 12 XRD test locations as the red circles

(b)

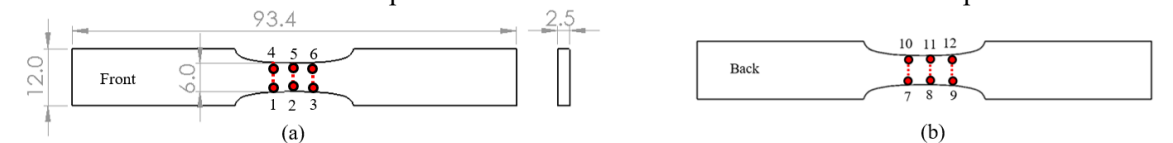
Fatigue damage was induced in the samples by applying fully reversed cyclic load ranging from 10% to 90% of the total average number of cycles to failure, in 10% increments. The testing was performed using an 810 MTS uniaxial servohydraulic machine, which has a  $\pm 50$  kN load capacity. Stress-controlled fatigue cycles were applied at stress amplitude of 200 MPa in a fully reversed mode (R = -1). Based on the preliminary tests and a log-normal distribution of fatigue life, the estimated mean total life was 150,220 load cycles, with a standard deviation of 34,462, based on 27 fatigue tests.

## 2.2 X-Ray diffraction measurements

X-ray diffraction analysis was performed on each fatigue sample using a Bruker D8-Discover diffractometer equipped with a VÅNTEC-500 area detector with a radius of 135 mm. Cu-K $\alpha$  radiation ( $\lambda = 1.5406$ Å) was used, with the X-ray tube operating at 40 kV and 40 mA. The collimator size was 2.0 mm, and each measurement included 24 diffraction images taken between 30° and 150° at 5° intervals. The exposure time for each image was 40 seconds, resulting in a total scan time of 16 minutes. From each scan, 9 distinct diffraction peaks were generated, and for each peak, 17 parameters were extracted. These parameters are observation max, d observation max, FWHM, chord middle, d chord middle, integral breadth, gravity center, d gravity center, raw area, net area, crystal size, left and right intensities, gross intensity, net height, signal/noise ratio, and peak/background ratio. As a result, each XRD test produced 153 data. The parameters starting with "d" (e.g., d observation max, d chord middle, and d gravity center) represent the interplanar spacing calculated from the corresponding  $2\theta$  values using Bragg's law equation [2].

#### 2.3 Dataset Formation

The structured data obtained from XRD peak profile analysis was compiled into a comprehensive dataset. Each record in the dataset contains 153 numerical parameters extracted from nine diffraction peaks, including FWHM, integral breadth, peak area, position, and shape descriptors. Additionally, the dataset includes the corresponding fatigue damage level of the specimen, expressed as a percentage of total number of cycles to the average final failure, and the spatial location of each XRD measurement relative to the center of mass of the dog-bone sample. For every specimen, measurements were performed at 12 different positions as shown in



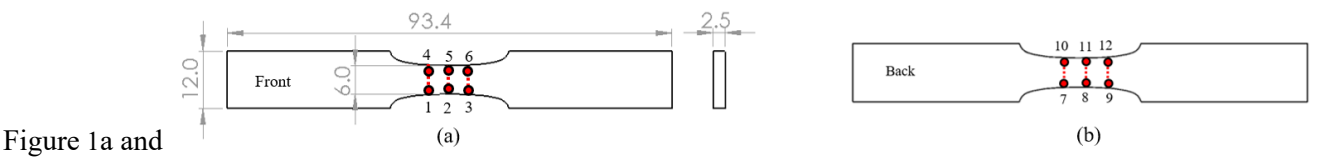


Figure 1b, enabling the spatial mapping of damage evolution. Raw diffraction images corresponding to each measurement were also archived in the dataset. An example of these kinds of images is shown in Figure 2a. The location of these peaks and their associated crystallographic planes are also presented in Figure 2b.

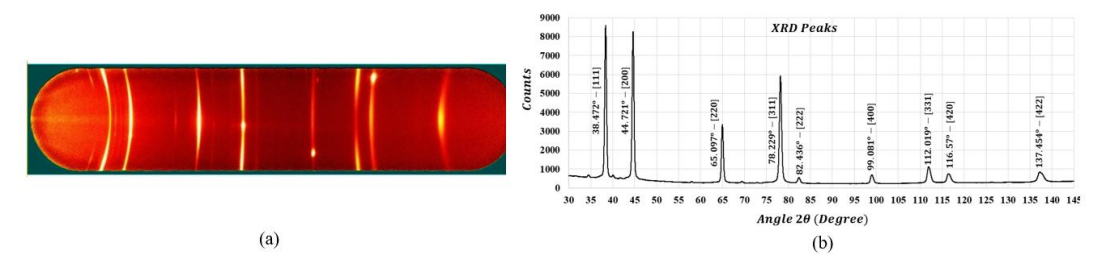


Figure 2: (a) Raw XRD diffraction image for AA6061-T6 samples, (b) The location and the Miller indices of the corresponding planes of the 9 peaks in the diffraction pattern of AA6061-T6

## 2.4 Dislocation Density Estimation via Williamson-Hall Method

To estimate dislocation density, the Williamson–Hall (WH) method was applied. This method separates the effects of crystallite size and lattice strain on peak broadening observed in XRD patterns. The WH equation is given by (1 Where  $\beta$  is the FWHM of the peak (in radians),  $\theta$  is the Bragg angle,  $\lambda$  is the X-ray wavelength, D is the average crystallite size,  $\varepsilon$  is the microstrain, and k is the shape factor (typically 0.9 [10]). Instrumental broadening was removed using relation for  $\beta$ , where  $\beta_{\varrho}$  and  $\beta_{i}$  are the FWHM before correction and the instrumental FWHM in radians, respectively.

$$4\varepsilon \sin \theta + \frac{k\lambda}{D} = \beta \cos \theta; \ \beta = \sqrt{(\beta_o - \beta_i)\sqrt{(\beta_o^2 - {\beta_i}^2)}}$$
 (1)

#### 3. Results and discussion

The first key result of this study is that, as expected, XRD peak characteristics respond measurably to fatigue-induced damage. For example, as shown in

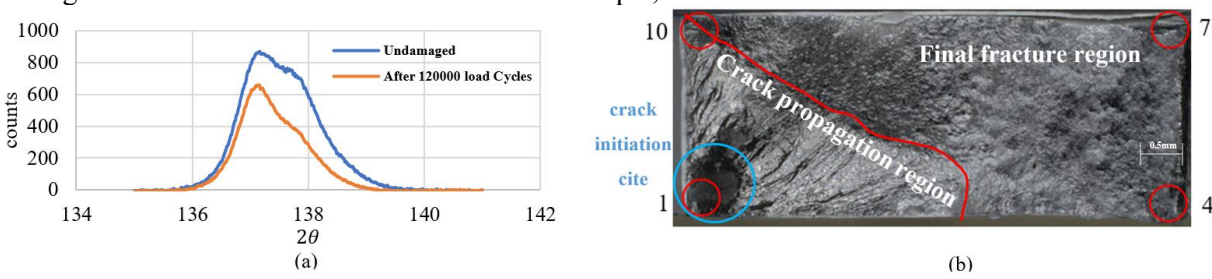


Figure 3a, the shape of peak 9 ([422] plane) changes significantly after damage is induced. The peak position (observation max) shifts from 137.315° to 137.149°, the FWHM decreases from 1.538° to 1.405°, and the maximum intensity (net height) drops from 22.66 to 17.65 counts per second after applying fatigue cycles equivalent to approximately 90% of the sample's final life of 132,853 cycles. These changes confirm that XRD is sensitive to fatigue damage and can reliably capture its progression.

Next, the WH method was applied to compare dislocation densities between undamaged samples and those that had fractured. A linear fit to the  $\beta\cos\theta$  versus  $\sin\theta$ , as shown in Figure 4, yields a slope related to the microstrain, and an intercept that corresponds to the crystallite size. Finally, the dislocation density  $\rho$  is estimated as  $\rho = \frac{14.4\varepsilon^2}{b^2}$ , where b is the Burgers vector, which is  $\frac{a}{\sqrt{2}}$  for FCC structures like aluminum, and a is  $4.05 \times 10^{-10}$  m [11]. The calculation of the dislocation density  $\rho$  is shown in Figure 4 as well.

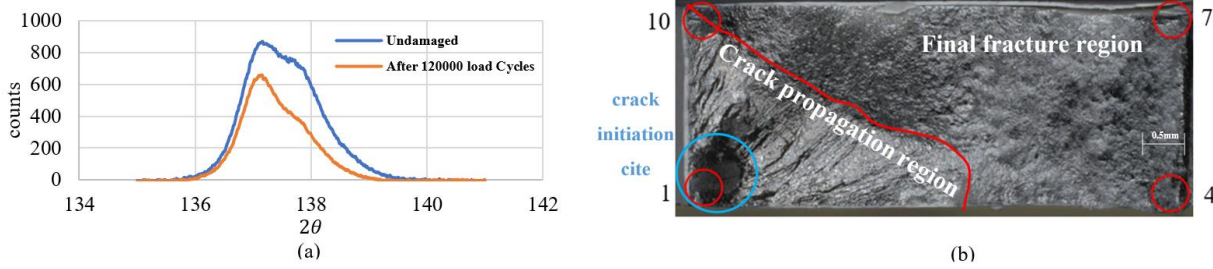


Figure 3: (a) Changes of peak 9 of AA6061-T6 before and after damage, (b) The fracture surface of one of the samples.

Location numbers are based on

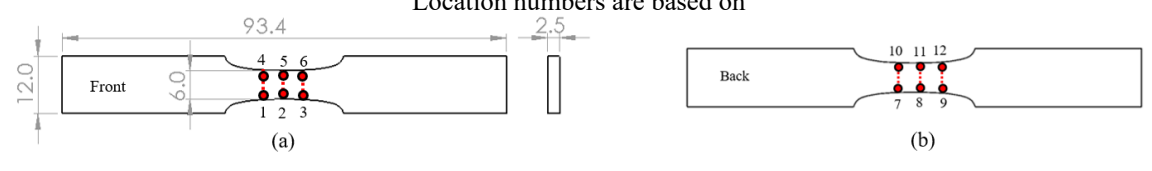


Figure 1.

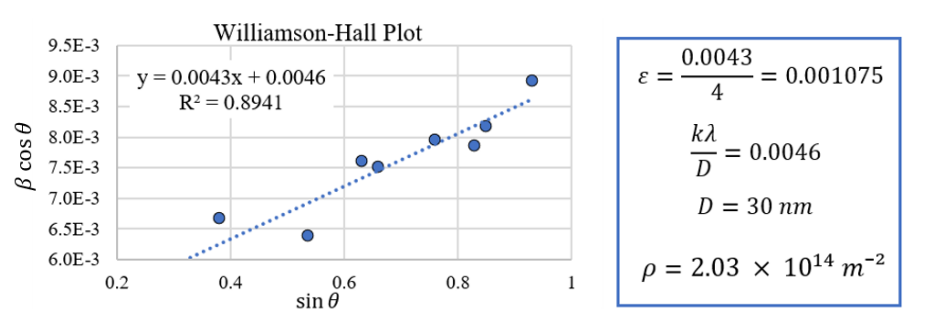


Figure 4: Williamson-Hall plot for one of the tests on AA6061-T6 samples. Solid blue circles representing the 9 peaks and the dash line is the linear fit, with the equation shown on the plot.

Although the current set of tests did not reveal a clear linear correlation between dislocation density and damage level across all samples, a consistent trend was observed: the average dislocation density increased from about  $1 \times 10^{14} \, m^{-2}$  in undamaged samples to about  $2 \times 10^{14} \, m^{-2}$  in fractured specimens. This indicates that while dislocation density may not scale linearly during damage, it approximately doubles after failure, highlighting its potential as a late-stage damage indicator. Finally, post-fracture surface of one of the samples is shown in

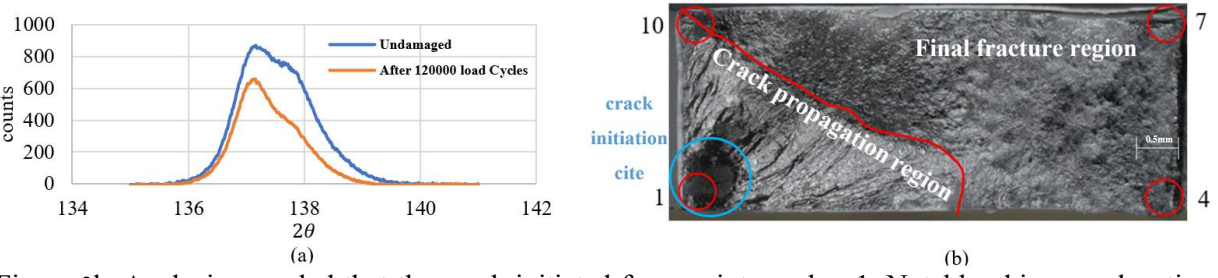


Figure 3b. Analysis revealed that the crack initiated from point number 1. Notably, this same location has the highest dislocation density in the pre-failure measurements (at 76% cycles of the final life). The value of the dislocation densities of the points 1,4,7, and 10 were  $2.14 \times 10^{14} \, m^{-2}$ ,  $1.05 \times 10^{14} \, m^{-2}$ ,  $1.05 \times 10^{13} \, m^{-2}$ , and  $1.05 \times 10^{13} \, m^{-2}$ , and  $1.05 \times 10^{13} \, m^{-2}$ , respectively. This finding supports the hypothesis that local dislocation density increases are predictive of impending crack initiation sites.

#### 4. Conclusion

This study investigated fatigue-induced microstructural changes in AA6061-T6 through extensive X-ray diffraction (XRD) measurements and derived several key findings. First, a clear difference in dislocation density was observed between undamaged and fractured samples, with average values nearly doubling from  $\sim 1 \times 10^{14}$  m<sup>-2</sup> to  $\sim 2 \times 10^{14}$  m<sup>-2</sup>. Second, noticeable changes in diffraction peak characteristics were detected under fatigue loading, including peak broadening, intensity reduction, and peak position shifts, confirming the sensitivity of XRD to damage evolution. Third, the initiation site of fatigue cracks coincided with the location of maximum dislocation density measured prior to failure, highlighting the predictive capability of localized dislocation density analysis. Taken together, these results demonstrate

that a strong relationship exists between the extent of fatigue damage in AA6061-T6 components and the corresponding XRD responses. However, this relationship is not yet fully established and requires further investigation to be comprehensively validated. As emphasized throughout this work, the value of XRD lies not only in tracking individual parameters such as FWHM but in leveraging the full spectrum of information embedded in both numerical features and raw diffraction images. To this end, all extracted peak parameters (153 per scan) together with the corresponding raw images have been systematically stored in a curated dataset. Looking forward, this dataset establishes the foundation for future machine learning applications. By integrating tabular data and raw diffraction images, both classical models (e.g., Random Forest, XGBoost) and deep learning approaches (e.g., convolutional neural networks) can be explored to enhance predictive capabilities and provide explainable insights into fatigue life estimation. Ultimately, this combined experimental—computational framework supports the development of targeted cold spray remanufacturing strategies, enabling cost reduction, material preservation, and improved sustainability.

## 5. Acknowledgments

The authors gratefully acknowledge the financial support from the Natural Sciences and Engineering Research Council of Canada (NSERC) through the ALLRP 577125–22 Alliance Missions grant, as well as facilities funds provided by the Canadian Foundation for Innovation through the Innovation Fund CFI-IF-43034 grant.

## 6. Conflicts of interest

The authors declare no conflicts of interest.

## 7. Statement on generative artificial intelligence usage

In the preparation of this manuscript, ChatGPT was used solely for language copy-editing purposes. The tool was applied to grammar refinement and increased fluency, and all AI-generated content has been thoroughly reviewed and edited by the authors to ensure originality and accuracy. We, the authors, affirm full authorship of the final text and accept complete responsibility for its content.

#### 8. References

- [1] Villafuerte J. Modern Cold Spray: Materials, Process, and Applications. Modern Cold Spray. 2015.
- [2] Bragg WH, Bragg WL. The reflection of X-rays by crystals. Proceedings of the Royal Society of London Series A, Containing Papers of a Mathematical and Physical Character. 1913;88(605):428-38.
- [3] Taira S., Honda K. X-ray Investigation on the Fatigue Damage of Metals. Bulletin of JSME. 1961;4(14):230-7.
- [4] Taira S. X-ray-diffraction approach for studies on fatigue and creep: The philosophy of the application of the X-ray-diffraction approach for studies on the mechanical behavior of materials is discussed by taking cases of studies of fatigue and creep as examples. Experimental Mechanics. 1973;13:449-63.
- [5] Pangborn RN, Weissmann S, Kramer IR. Dislocation distribution and prediction of fatigue damage. Metallurgical Transactions A. 1981;12(1):109-20.
- [6] Zamrik SY, Pangborn RN. Fatigue damage assessment using x-ray diffraction and life prediction methodology. Nuclear Engineering and Design. 1989;116(3):407-13.
- [7] Kim S-H, Cho S-S, Park J-H. Prediction of Fatigue Life in 2024-73 Aluminum Using X-ray half-value breadth. International Journal of Precision Engineering and Manufacturing. 2002;3(2):78-86.
- [8] Pinheiro B, Lesage J, Pasqualino I, Benseddiq N, Bemporad E, editors. Toward a Fatigue Life Assessment of Steel Pipes Based on X-Ray Diffraction Measurements. International Conference on Offshore Mechanics and Arctic Engineering; 2015: American Society of Mechanical Engineers.
- [9] Drumond G, Pinheiro B, Pasqualino I, Roudet F, Chicot D. Fatigue Life Prediction of Steel Pipelines Based on X-ray Diffraction Analyses. Journal of Materials Engineering and Performance. 2022;31(1):801-13.
- [10] B.D. Cullity SRS. Elements of X-Ray Diffraction. Third Edition ed: Pearson; 2014.